

ORIGINAL ARTICLE

Ligament Tissue Engineering Using a Novel Porous Polycaprolactone Fumarate Scaffold and Adipose Tissue-Derived Mesenchymal Stem Cells Grown in Platelet Lysate

Eric R. Wagner, MD,¹ Dalibel Bravo, MD,¹ Mahrokh Dadsetan, PhD,² Scott M. Riester, MD,² Steven Chase, BS,² Jennifer J. Westendorf, PhD,¹ Allan B. Dietz, PhD,² Andre J. van Wijnen, PhD,² Michael J. Yaszemski, MD, PhD,² and Sanjeev Kakar, MD¹

Purpose: Surgical reconstruction of intra-articular ligament injuries is hampered by the poor regenerative potential of the tissue. We hypothesized that a novel composite polymer “neoligament” seeded with progenitor cells and growth factors would be effective in regenerating native ligamentous tissue.

Methods: We synthesized a fumarate-derivative of polycaprolactone fumarate (PCLF) to create macro-porous scaffolds to allow cell–cell communication and nutrient flow. Clinical grade human adipose tissue-derived human mesenchymal stem cells (AMSCs) were cultured in 5% human platelet lysate (PL) and seeded on scaffolds using a dynamic bioreactor. Cell growth, viability, and differentiation were examined using metabolic assays and immunostaining for ligament-related markers (e.g., glycosaminoglycans [GAGs], alkaline phosphatase [ALP], collagens, and tenascin-C).

Results: AMSCs seeded on three-dimensional (3D) PCLF scaffolds remain viable for at least 2 weeks with proliferating cells filling the pores. AMSC proliferation rates increased in PL compared to fetal bovine serum (FBS) ($p < 0.05$). Cells had a low baseline expression of ALP and GAG, but increased expression of total collagen when induced by the ligament and tenogenic growth factor fibroblast growth factor 2 (FGF-2), especially when cultured in the presence of PL ($p < 0.01$) instead of FBS ($p < 0.05$). FGF-2 and PL also significantly increased immunostaining of tenascin-C and collagen at 2 and 4 weeks compared with human fibroblasts.

Summary: Our results demonstrate that AMSCs proliferate and eventually produce a collagen-rich extracellular matrix on porous PCLF scaffolds. This novel scaffold has potential in stem cell engineering and ligament regeneration.

Introduction

INTRARTICULAR LIGAMENT injuries are becoming increasingly common and if left untreated can lead to abnormal articular loading and ultimately progressive degenerative changes of the joint.¹ From an economic perspective, it is estimated that the annual cost of osteoarthritis in the United States is \$82 billion.² The poor healing potential of these ligaments is in part due to the poor healing potential from the intrasynovial location with limited intrinsic healing ability.³ Tissue engineering aims to develop a specialized scaffold with a biologically functional extracellular matrix (ECM) and biomechanical properties suitable for enhancing regenerative repair. While scaffolds provide an initial

framework for stability and guiding tissue ingrowth, ideal ligament scaffolds must create a framework for tissue ingrowth, meet the initial mechanical demands, degrade with time, and most importantly achieve functional integration of soft ligament tissues.^{4–6}

Strategies in ligament engineering combine natural or synthetic polymer technology with biological regeneration, such as growth factors and stem cells. However, there has been limited success in joining the two strategies in part because the hydrophobic and acidic nature of synthetic scaffolds prevents cellular adhesion and induces local inflammation. Furthermore, there have been issues with cell seeding and maintaining mechanical integrity of decellularized scaffolds, and the inherent low mechanical strength of

¹Department of Orthopedic Surgery, Mayo Clinic, Rochester, Minnesota.

²Department of Orthopedic Surgery and Biomedical Engineering, Mayo Clinic College of Medicine, Rochester, Minnesota.

collagen scaffolds.^{7–11} Utilizing both strategies is critical because manipulation of mesenchymal cell differentiation has shown promise in regeneration of native tissue.^{12–14}

Currently, there is considerable interest in defining ideal ligament scaffolds and therefore our goal has been to create a novel engineered neoligament tissue. In this study, we have examined growth of mesenchymal cells on a synthetic scaffold prepared from biodegradable polymers in the presence of ligament-related growth factors to assess whether such biologically enhanced scaffolds have the potential to restore native ligamentous tissue and architecture. Specifically, our methodology utilizes the biocompatibility of polycaprolactone (PCL) cross-linked using the natural glycolytic metabolite fumarate (polycaprolactone fumarate [PCLF]) to create a novel scaffold with interconnected channels. We show that this scaffold permits proliferation of mesenchymal stem cells in the presence of platelet lysate (PL) and exhibits deposition of a collagen-rich ECM upon administration of fibroblast growth factor 2 (FGF-2).

Materials and Methods

Synthesis of PCLF

All chemicals were purchased from Aldrich or Fisher Chemicals, unless otherwise noted. PCLF was synthesized as previously described^{15–18} (Fig. 1). To eliminate the toxic degradation product diethylene glycol, PCLF was synthesized using propylene glycol and glycerol.¹⁹ Briefly, the polymer compositions and molecular weights were characterized by ¹H NMR spectroscopy and gel permeation chromatography. PCLF (3.0 g) was dissolved in 1 mL of methylene chloride. The photo-initiator Irgacure 819 (0.3 g) was dissolved in 3 mL of methylene chloride, and 300 μ L

was added to the PCLF and gently vortexed to form a viscous homogenous solution.

Scaffolds were designed to mimic the tendon size of rabbit anterior cruciate ligament (ACL) (4 \times 10 mm) and to have square pores (500 \times 500 μ m or 750 \times 750 μ m) to allow cell–cell communication and nutrient flow. Porous scaffold molds were designed using SolidWorks CAD software (3D CAD Solutions) and printed using a SolidScape 3D printer (SolidScape Lab 3D). The PCLF and cross-linker solution was injected over the sacrificial molds created by the SolidScape printer. The molds containing the PCLF solution was then cured using UV cross-linking chamber (3D system) for 1 h. After removal from the chambers, the molds were removed from the scaffolds using a mixture of methanol and acetone washes over a period of 3 days.

Toxicity protocols

After removing the molds from the scaffolds, the scaffolds underwent an analysis of multiple toxicity protocols involving hydrophobic solvents like methylene chloride, ethanol, and acetone. These washes involved a series of 12-h washes involving a combination of different combinations of these solvents. Briefly, the ethanol-based protocol involved washing the scaffolds in 100%, 90%, and 70% ethanol with interspersed immersions of phosphate buffered solution (PBS). The acetone-based regimen utilized two separate 12-h washes in 75:25 acetone:ethanol and 50:50 (v/v) acetone:ethanol, followed by washing for 24 h in 70% ethanol solution. The methylene chloride-based protocol involved 12-h washes of scaffolds in, respectively, 50:50 (v/v) methylene chloride:acetone, 50:50 (v/v) methylene chloride:ethanol, and 50:50 (v/v) acetone:ethanol, followed by 24 h in 70% ethanol.

Scanning electron microscopy and microCT

Images of the scaffold were obtained using the Hitachi 4700 field emission spectrometer. The PCLF scaffolds were fixed with 2.5% glutaraldehyde solution for 20 min, washed with PBS and dehydrated in a series of graded aqueous ethanol solutions.

In vitro cell culture

All cells used in these experiments were initially cultured in advanced Modification of Eagle's Media (aMEM; Invitrogen), supplemented with 10% fetal bovine serum (FBS), 1% penicillin/streptomycin, and L-glutamine (Invitrogen), standardized to a pH of 7.2. Cells before and after seeding on scaffolds were incubated at 37°C, with media changed every 2 days. For the collagen and immunofluorescence assays, cells were also cultured with or without FGF-2 at a concentration of 10 ng/mL.

Platelet lysate

For the proliferation, viability, and differentiation experiments, comparison were made between the control (aMEM with 10% FBS) and a media based on PL. The PL media included aMEM with 5% PL, 1% penicillin/streptomycin, and L-glutamine. PL was procured according to Good Manufacturing Practice (GMP)-adherent protocols as previously described.²⁰ Briefly, 500 distinct platelet donors from the Mayo Clinic Blood Bank were lysed into lots containing 8–12

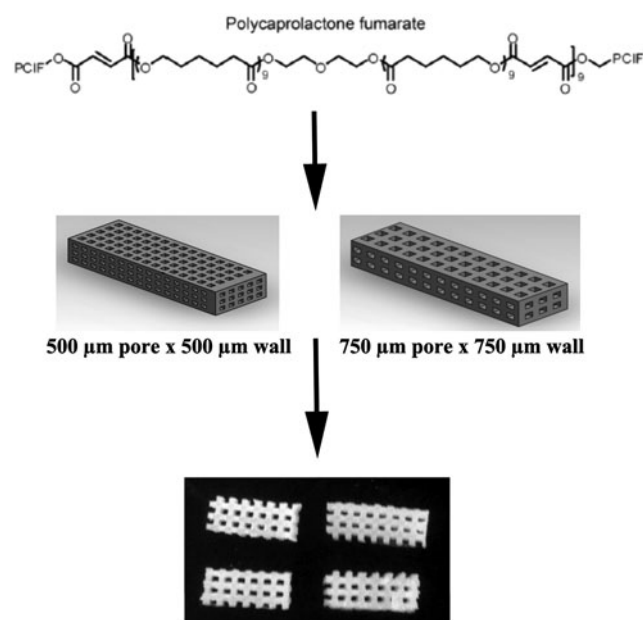


FIG. 1. Polycaprolactone fumarate (PCLF) synthesis. PCLF scaffolds were made using ultraviolet cross-linking. The scaffold geometry was designed using CAD software and printed using a 3D printer, with large interconnected pores to allow tissue infiltration and cell–cell communication.

donors. The facility used to generate the PL were subject to strict environmental monitoring for adherence to GMP standards, with quality assurance measures taken to the freeze-thaw manufacturing approach.²¹

Human adipocyte-derived mesenchymal stem cell and ACL fibroblast isolation

Adipocyte-derived mesenchymal stem cells (AMSCs) and fibroblasts were isolated and cultured as previously described²⁰ using protocols compliant with recommendations of the Mayo Clinic institutional review board (IRB). Briefly, human adipose tissue was obtained from different anatomic compartments in patients undergoing multiple general surgical operations. The tissue was subsequently minced with scalpels, incubated in 0.075% collagenase type I (Worthington Biochemical) for 90 min at 37°C, centrifuged at 500 *g* for 10 min and passed through a 70 µm cell strainer (BD Biosciences). For fibroblast isolation, intrasynovial human ACL tissue was minced for 15–20 min, incubated in 0.1% collagenase type 1 and collagenase D (Roche) for 90 min at 37°C, centrifuged at 500 *g* for 10 min, and passed through sterile 70 µm cell strainers. Expansion media was aMEM with either 10% FBS or 5% PL, 100 U/mL penicillin, and 2 mM L-glutamine.

Dynamic rotational bioreactor cell seeding and attachment

After fabrication of the macroporous PCLF scaffolds, the scaffolds underwent a toxicity protocol, followed by disinfection with ethanol washes and sterile PBS. Cell suspensions with a concentration of 1 million cells per milliliter of media were seeded onto the scaffolds using one of three seeding strategies. In the static group, a cell suspension of 1 million cells in media was seeded by directly pipetting the solution onto the scaffolds in a slow, deliberate manner over a 5-min period. The suspension group involved deliberately pipetting the cells onto the scaffold and immersing seeded scaffolds in the same media containing 1 million cells per mL for 12 h. In the dynamic group, 12 scaffolds were placed inside a dynamic rotational bioreactor (Synthecon) containing 12 mL of media with 1 million cells per mL. The gravitational component was removed through a constant rotational force applied at 18 rpm for 18 h. Subsequently, the scaffolds were removed and incubated in static 24-well cell culture plates. The number of cells attached to scaffolds in each of the treatment groups were quantified using the MTS Cell Proliferation Assay (Promega Corporation) and by counting for the number of viable cells stained with Trypan Blue.

Proliferation, toxicity, and viability assays

MTS and cell counting assays were used for cytotoxicity and proliferation assays. For the toxicity assay, the scaffolds underwent one of three solvent toxicity protocols as mentioned above, based on ethanol, acetone, or methylene chloride. After disinfection with ethanol washes, the cells were seeded on to the scaffolds using direct pipetting and suspending in a cell solution. After 24 h the scaffolds were removed, washed with PBS, and placed in a new 24-well plate. The MTS Cell Proliferation Assay (Promega Corporation) was used to quantify the mitochondrial activity.

Cells from the initial cell solution not in contact with the scaffolds were used as positive control. In a separate toxicity cell counting assay, the cells were quantified after the cells were trypsinized off the scaffolds, viable cells stained with trypan blue and counted using a hexameter.²²

Cellular proliferation was quantified for using both MTS assays and cell counting, as previously described.²² Comparisons were made between cells cultured in FBS and PL-based media, and the cells culture on scaffolds with pore sizes of 500 and 750 µm at days 1, 3, 5, 7, and 14.²²

Cellular viability was assessed at days 1, 7, and 14, cell morphology and viability was examined using a Live/Dead Kit (Molecular Probes). Viable living cells (green) were stained with calcein AM, while dead or apoptotic cells (red) were stained with ethidium bromide. The cells were visualized using confocal microscopy (Zeiss LSM 780; Zeiss).

Alkaline phosphatase activity and glycosaminoglycan assays

Baseline cell characterization was performed using alkaline phosphatase (ALP; Sigma) and glycosaminoglycan (GAG) assay, as previously described.²³ The cells were seeded and cultured in static 24-well culture dishes for 1, 7, and 14 days. The overall ALP activity was normalized to the total protein content present using the Bradford protein assay (Bio-Rad).

The GAG assays were performed at the same time points of 1, 7, and 14 days. Briefly, the scaffolds were rinsed with PBS before digestion in 50 µg per mL of proteinase K in 100 mM K₂HPO₄, pH 8.0 at 60°C for 16 h. At the end of the digestion, the proteinase K was inactivated at 90°C for 10 min. This solution was used for the GAG assay with Blyscan Glycosaminoglycan Assay Kit (Biocolor). The total GAG content was standardized by the total DNA content on each PCLF scaffold using the Picogreen Cell Proliferation Kit (Molecular Probes).

Total collagen assay

The total amount of secreted and deposited collagen on the PCLF scaffolds was quantified using the Sircol Collagen Dye Binding Assay Kit (Biocolor, Ltd.), as previously described.²⁴ This protocol is based on Sircol dye specific for collagen's Gly-X-Y helical structure, but not the unwound triple helix or other random similar chains. The total collagen amount was normalized using the total DNA content on each PCLF scaffold as determined by picogreen staining (Picogreen Cell Proliferation Kit; Molecular Probes).

Immunofluorescence staining

The deposition of collagen I, tenascin-C, and collagen III on PCLF scaffolds were visualized and quantified as previously described.²⁵ After the staining protocol, images of each scaffold were obtained using confocal microscopy (Zeiss LSM 780; Zeiss). Red signals represent the protein of interest, while blue represents the DAPI nuclear stain. The amount of Cy3 expression was quantified using Image J software.²⁶

Statistical analysis

A two-tailed Student's *t*-test was used to compare control groups in each respective assay with the individual experimental groups for toxicity, cell seeding, proliferation, GAG,

ALP, collagen, and immunofluorescence experiments. Results with $p < 0.05$ were deemed statistically significant.

Results

Toxicity analysis

The AMSCs were seeded on the scaffolds to test the toxicity associated with different solvent-based protocols. Due to the toxicity of the original starting materials, residuals monomers and uncross-linked PCLF must be removed using some combination of ethanol, methylene chloride, and/or acetone-based scaffold washes. AMSCs were seeded on to the scaffolds 24 h before the cytotoxicity evaluations. The number of living viable cells were significantly increased on scaffolds associated with the acetone-based or methylene chloride and acetone-based toxicity protocols, when compared to the ethanol only protocol ($p < 0.01$) (Fig. 2A). These two protocols maintained a comparable number of viable cells to the control wells, containing cells not seeded on a scaffold. Counting the number of viable cells after Trypan Blue staining demonstrated similar findings, with a higher number of viable cells on the scaffolds washed with acetone or methylene chloride and acetone-based protocols ($p < 0.01$) (Fig. 2B).

PCLF morphology

Polymer scaffold surface topography and pore size are one of many factors that influence cell attachment, sustained viability, and proliferation, in addition to tissue infiltration and ligament regeneration. The scanning electron microscopy (SEM) demonstrates rough surfaces along the PCLF surfaces lining the channels (Fig. 3). This roughness is in the order of tens of microns in size, which is sufficiently large to facilitate sustained cell attachment.

The pore size was measured using the SEM software, with measurements taken on multiple areas on all six surfaces of the scaffold. Figure 3A and B demonstrate the size of the interconnected pores, forming channels throughout the body of the scaffolds. We compared the theoretical pore and pillar size as designed through SolidWorks Software with the actual pore and pillar size after processing the scaffolds. The pore size of the scaffolds decreases between 16% and 12%, while the pillars lining the channels swell ~ 8 –15% beyond the

initial size. Regardless of the swelling, the scaffold channels remain very large: the 500-micron scaffolds maintain average pore sizes of ~ 420 microns, while the 750-micron scaffolds sustain pores of ~ 659 microns on average.

Scaffold static versus bioreactor cell seeding

Scaffolds were seeded with AMSCs using three different seeding protocols; direct pipetting (static group), pipetting and cell suspension (suspension group), and suspension in the dynamic bioreactor (bioreactor group). Figure 4 demonstrates the differences in the cell counting and MTS assays between different seeding groups. The most encouraging results show statistically significant improvement in cell attachment in the dynamic seeding group.

AMSC attachment, viability, and distribution

Cellular attachment and sustained viability are important considerations for the use of novel scaffolds in tissue engineering. Cell attachment 24 h after removal from the bioreactor was visualized with the Live/Dead Kit to stain the viable cells (green signal) and apoptotic cells (red signal) (Fig. 5). The cells appeared evenly distributed throughout all the scaffolds with both the 500 and 750-micron pore sizes. There did not appear to be any difference between the two different scaffold morphologies. The number of cells markedly increased after day 7 with cells infiltrating throughout the channels inside the body of the scaffolds in both groups. By day 14, the cells remained viable and continued to increase in number, as evidenced by complete coverage of cells throughout the surface and channels of the PCLF scaffold. Figure 5 displays representative images for scaffolds with 500 and 750-micron pore sizes at days 1, 7, and 14.

Cellular attachment and proliferation

In addition to assessing cellular viability, cellular attachment and proliferation were quantified over the 14-day incubation period by MTS and cell counting assays. At the end of each time point, comparisons in the number of viable cells were between PL and FBS, and scaffolds with pore sizes of 500 and 750 microns. There was no difference in initial cellular attachment 24 h in any of the treatment groups after seeding AMSCs using the dynamic bioreactor, as demonstrated by both

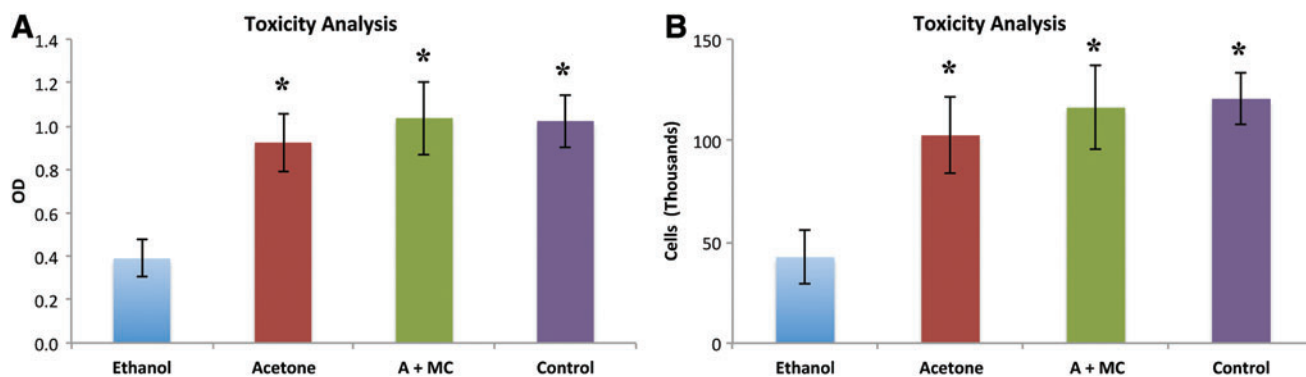
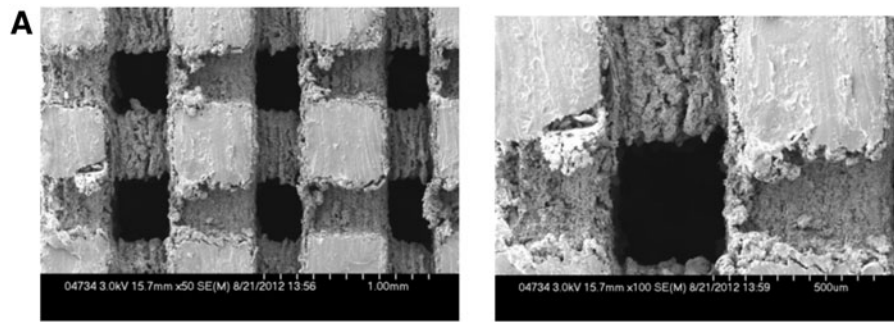
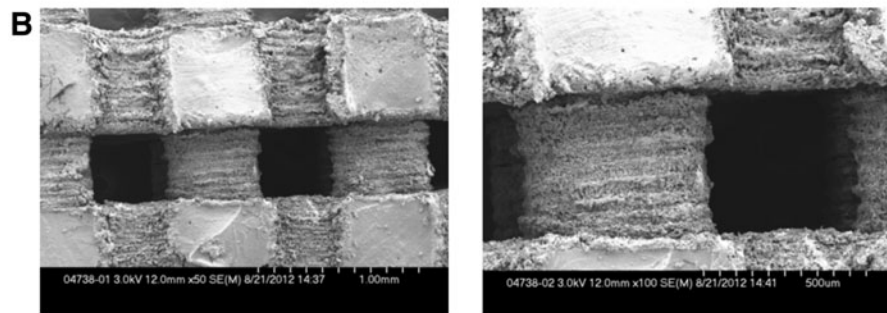


FIG. 2. Toxicity analysis. The cytotoxicity of the PCLF scaffolds after various toxicity removal protocols were tested utilizing the MTS (A) and cell counting assays (B). The protocols were based with ethanol, acetone, or acetone and methylene chloride, and were compared to a control group of cells for the initial solution not in contact with the scaffolds. * p -value < 0.05 when compared to ethanol alone. Color images available online at www.liebertpub.com/tea



Pore Size Change		
Initial Pore Size (um)	Actual Pore Size (um)	Percent Change
500	420 +/- 23	84%
750	659 +/- 32	88%



Pillar Size Change		
Initial Pillar Size (um)	Actual Pillar Size (um)	Percent Change
500	575 +/- 28	115%
750	810 +/- 17	108%

FIG. 3. MicroCT imaging of scaffolds. MicroCT images of the scaffolds demonstrating the large interconnected pores of the two scaffold sizes (500 and 750 microns) (A) and (B). There was minimal change in pore size after the toxicity and sterilization processing protocols.

MTS and cell counting assays (Fig. 6). AMSCs cultured on scaffolds in the presence of PL had a significantly increased rate in cellular proliferation compared to the AMSCs cultured in FBS media ($p < 0.05$) (Fig. 6A). There were no significant differences between scaffolds with 500 or 750 micron pore

sizes. However, cell counting demonstrated that after an initial increase in both groups for the first 3 days, the cells are not released by trypsin on our scaffolds by day 7 under our experimental conditions (Fig. 6B). The cells appear to remain adherent to the scaffolds by day 14 in all groups.

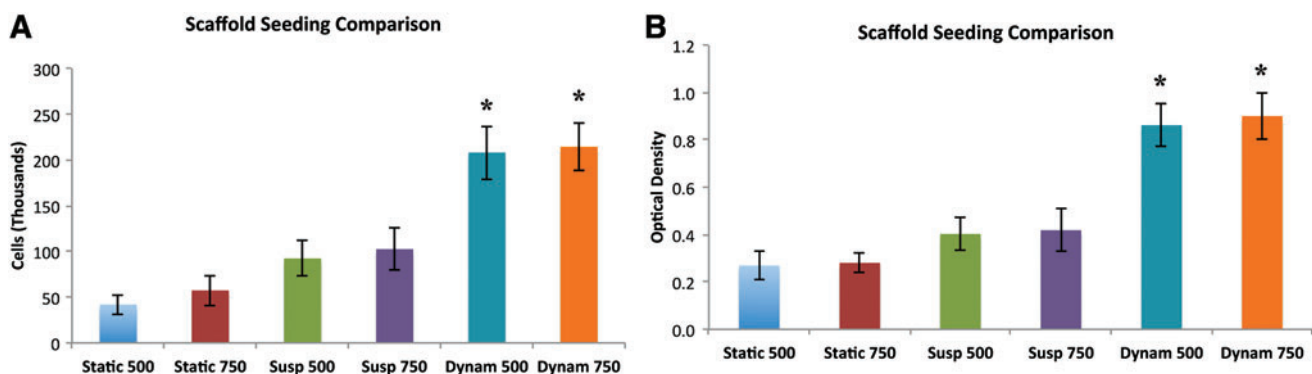
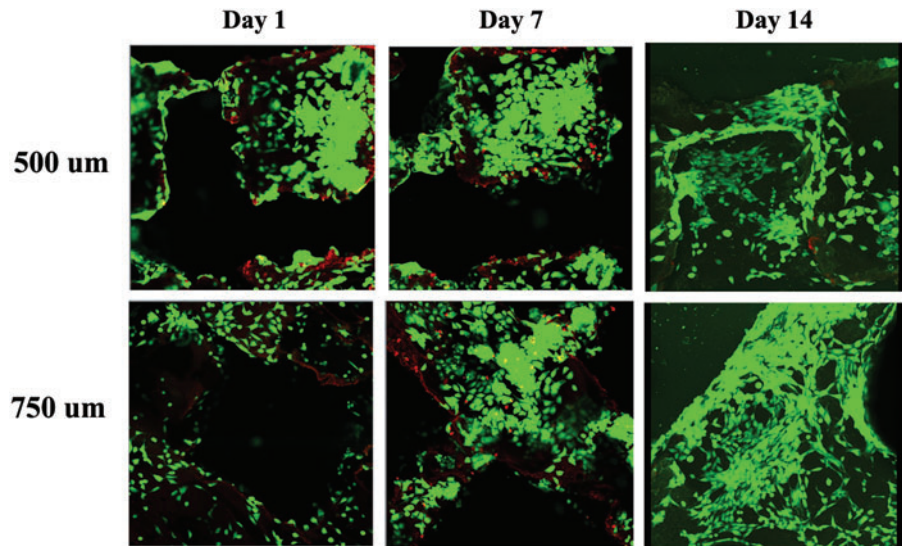


FIG. 4. Scaffold seeding comparison. A seeding comparison was performed between static (pipetting directly onto the scaffolds), suspension (immersing the scaffolds in suspensions containing the cells), or dynamic seeding (in the rotating bioreactor). The bioreactor, at a speed removing the gravitational component, had the highest rate of cell seeding as determined using MTS (A) and cell counting assays (B). * p -value < 0.05 when compared to static group. Color images available online at www.liebertpub.com/tea

FIG. 5. Cellular viability with live/dead assay. After seeding with the dynamic bioreactor, stem cells were cultured for 14 days, demonstrating proliferation and invasion into the pores. *Green*—live cells. *Red*—cells undergoing apoptosis. Color images available online at www.liebertpub.com/tea



AMSC, GAG, and ALP expression

It is not clear whether the interaction of AMSCs with PCLF affects the phenotype and multilineage differentiation potential of these adipose tissue-derived stem cells. To assess whether the cells begin to differentiate down chondrogenic or osteogenic pathways when cultured on the cells, the expression of the chondrogenic marker GAG and the osteogenic marker ALP was quantified. PL by itself does not induce osteogenic or chondrogenic differentiation of these cells.²⁰ The expression of GAG and ALP by the AMSCs on the PCLF scaffolds cultured in FBS or PL media on scaffolds with pore sizes of 750 microns were quantified at days 1, 7, and 14. The results obtained with AMSCs were compared to observations with chondrocytes and osteoblasts as positive controls.

There was no significant difference in expression of GAG between AMSCs on scaffolds cultured in PL or FBS, and no increase in GAG expression by the cells over the 14-day period when standardized by total DNA content (Fig. 7A). However, total GAG deposition was significantly reduced in the AMSCs when compared to the chondrocyte controls. Similar to GAG expression, total ALP expression normalized to total protein content did not increase throughout the 14-day time period (Fig. 7B). Although PL slightly increased the

expression of ALP when compared to FBS, this minor difference was significantly lower in both groups than the baseline ALP expression from the control group osteoblasts ($p < 0.05$). These biomarker results suggest that AMSCs cultured on PCLF scaffolds do not adopt overt osteogenic or chondrogenic phenotypes under our experimental conditions.

AMSC total collagen expression

The amount of total secreted and deposited collagen by the AMSCs along the scaffolds was assessed using the Sircol Total Collagen Assay. This is a preliminary nonspecific marker for fibrogenic differentiation and an indication of ECM formation.²⁴ The total collagen production by the AMSCs increased throughout the 28-day experiment (Fig. 8). The increase in collagen ECM formation became apparent at day 7 and increased until day 28. Furthermore, cells cultured in PL media had higher production of collagen at days 14 and 28 ($p < 0.05$) (Fig. 8A). When FGF-2 was added to both PL and FBS media, there was a significant increase in collagen production by the AMSCs on the scaffolds ($p < 0.01$). This increased in collagen ECM is consistent with the tight attachment of cells after the first week of growth when cells become quite resistant to trypsin digestion.

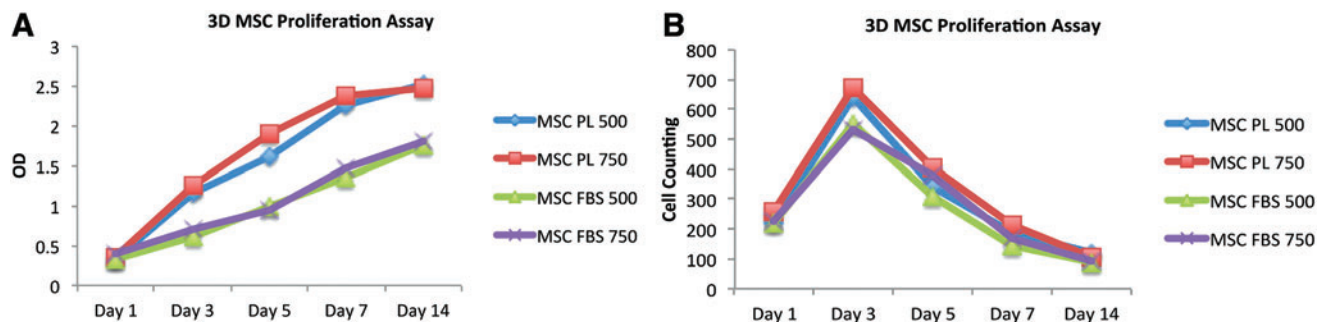


FIG. 6. Cellular proliferation assay. Stem cells were cultured on the scaffolds in the presence of fetal bovine serum (FBS) or platelet lysate (PL). Although the MTS assays indicated that the cells continued to proliferate beyond day 14 (A), the cells were not able to be trypsinized off the scaffolds beyond day 5, possibly indicating their attachments were resistant to trypsin (B). Color images available online at www.liebertpub.com/tea

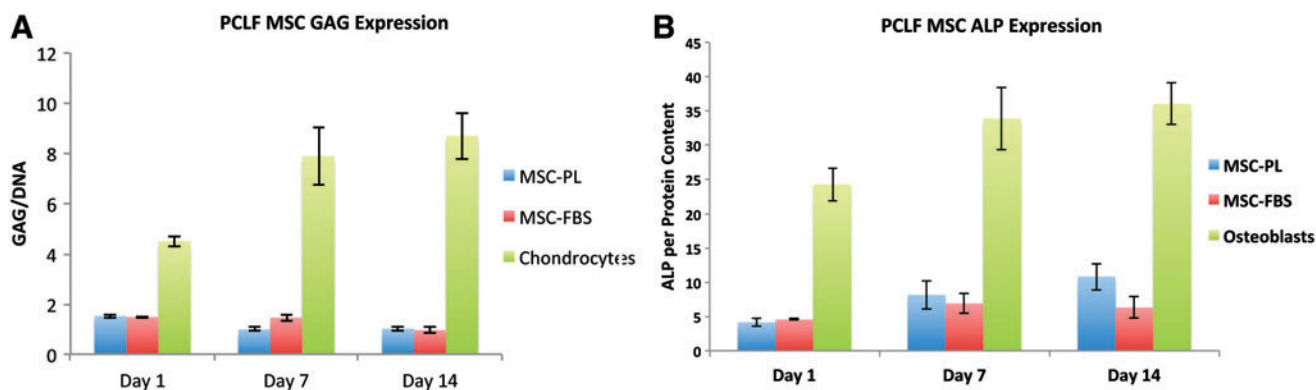


FIG. 7. Osteogenic and chondrogenic assay. The chondrocyte differentiation marker glycosaminoglycan (GAG) (A) and the osteogenic differentiation marker alkaline phosphatase (ALP) (B) were assessed at different time points, demonstrating the stem cells did not differentiate on the scaffolds in the presence of PL or FBS. Color images available online at www.liebertpub.com/tea

Immunostaining for ligament differentiation markers

The expression of ECM markers for ligament differentiation were analyzed using immunostaining for collagen I, tenascin-C, and collagen III, with Cy3 (red signal) expression for each protein. The DAPI nuclear counterstaining represents the blue signal. After seeding with the dynamic bioreactors, the scaffolds were cultured in the presence of FBS alone (FBS), PL alone (PL), FBS and FGF (FGF), and PL plus FGF-2 (PL+FGF), with human ACL fibroblasts as a positive control. The cells were cultured for 14 and 28 days before IHS staining was visualized by confocal microscopy (Fig. 9A).

By 14 days, there was a significant increase in expression of tenascin-C in the FGF and PL+FGF groups, when compared with the FBS alone ($p < 0.05$) (Fig. 9B). The expression of PL+FGF was comparable to the baseline tenascin-C matrix protein expression from the fibroblasts. The ECM containing the tenascin-C protein appeared to begin to cover most of the scaffold surface in both the PL+FGF and fibroblast groups. By 28 days, the expression of tenascin-C in the ECM was significantly increased in the PL+FGF group and the positive control fibroblast group (Fig. 9A). In addition to the PL+FGF and fibroblast groups, the PL and FGF groups also had increased expression of tenascin-C when compared with FBS alone ($p < 0.05$). At

this time point, the ECM containing the tenascin-C of the PL+FGF and fibroblast groups covered the entire scaffold surface area, including infiltrating throughout the channels within the body of the PCLF scaffolds.

The expression of collagen I was also significantly increased in the PL+FGF and FGF groups when compared to FBS alone at 14 days ($p < 0.05$) (Fig. 9B). Similar to tenascin-C, the expression of collagen I in the ECM produced by AMSCs in the PL+FGF group were comparable to fibroblasts. At 28 days, the scaffolds containing AMSCs cultured in the PL, FGF, and PL+FGF groups all had significantly increased expression of collagen I compared with FBS ($p < 0.05$). The matrices of the PL+FGF and fibroblast groups contained a marked amount of interconnected cells expressing collagen I covering most of the surface of the scaffolds, including throughout the inner pores (representative images in Fig. 9A). This was seen to a lesser extent in the FGF group as well.

The expression of collagen III was not as striking as the other two ECM markers. Collagen III is thought of as a nonspecific marker of fibrogenic differentiation.²⁴ Although at day 14 the expression of collagen III increased in the FGF, PL+FGF, and fibroblast groups compared with FBS alone, this difference was not as striking as the other ECM markers ($p < 0.05$). Furthermore, while this increased

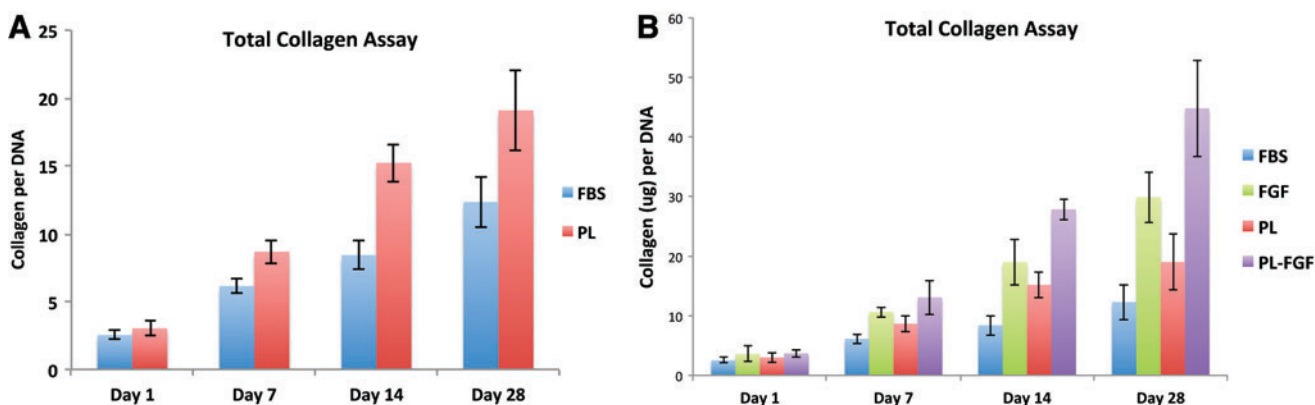


FIG. 8. Total collagen assay. Total collagen levels produced by stem cells grown on scaffolds in PL and FBS demonstrated the cells produced increasing levels of collagen through 4 weeks, both in the absence (A) and the presence (B) of FGF. Color images available online at www.liebertpub.com/tea

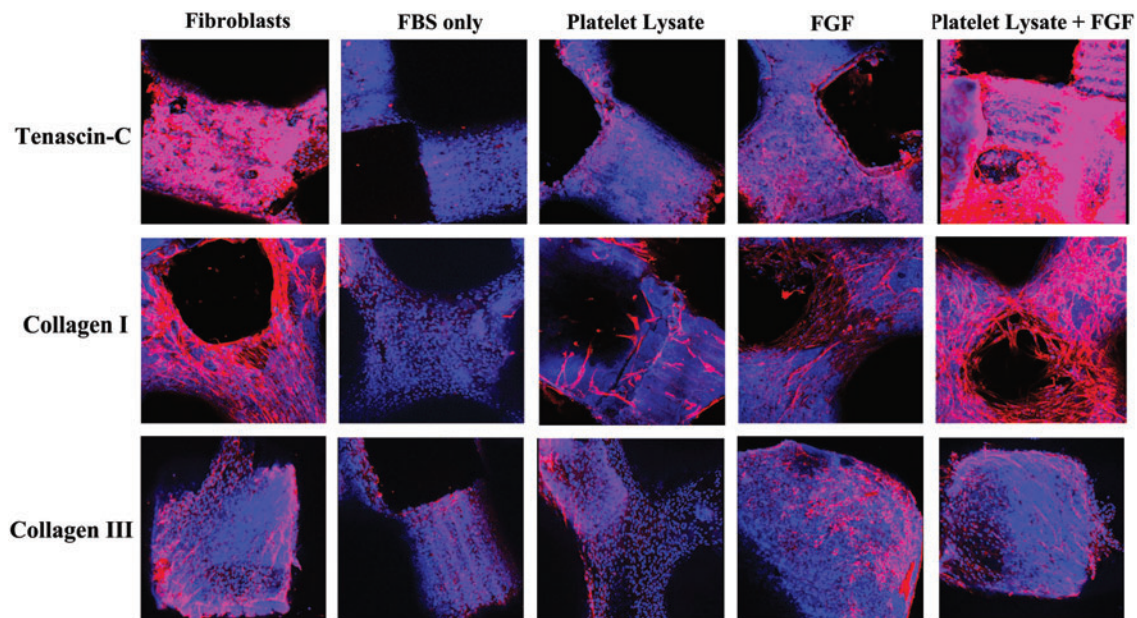


FIG. 9. Ligamentous differentiation live immunostaining assay. The stem cells were cultured on scaffolds in the presence of FBS only, PL, fibroblast growth factor (FGF) in FBS (FGF), or PL and FGF. The positive control was anterior cruciate ligaments (ACL) fibroblasts. The *red* staining represents cells expressing the different marker ligamentous differentiation markers. The *blue* staining represents the live cells covering the scaffolds (DAPI nuclear staining). Color images available online at www.liebertpub.com/tea

expression continued at 28 days, the FBS only group did have a relatively increased expression of collagen III compared with the other two ECM markers. Additionally, there was minimal difference between the expression of collagen III, when comparing the FGF, PL+FGF, and fibroblast groups (Fig. 9A).

Discussion

Intrasynovial ligament injuries are difficult to treat due to their poor healing capacity. These injuries predispose patients to recurrent pain and joint instability, chondral injuries, and early onset osteoarthritis.^{27–30} These injuries are usually treated with surgical reconstruction using allograft or autograft tendons. Although the initial strength is satisfactory with this technique, donor site morbidity, loss of structural integrity with time, and unfavorable immunogenic response when allograft tendons are used make this strategy less than ideal.^{31,32} Therefore, there has been a focus to create a neoligament with stable initial biomechanical properties that overtime will resemble the native ligament. Three main tissue-engineering strategies have been employed: (1) decellularized allograft, (2) natural polymer, or (3) synthetic polymer scaffold. When used alone, these acellular scaffolds might meet the mechanical demands but lack both cellular conductive and inductive properties. However, when used in combination with mesenchymal progenitor cells and growth factors, they represent a promising solution to native ligamentous regeneration.

We created a novel synthetic polymer scaffold that is able to be seeded with progenitor and mature fibroblasts, which in combination with growth factors were able to be induced to express a ligament-like matrix covering the scaffolds. Our goal was to create a scaffold with four essential properties for

ligament engineering: (1) Biocompatible scaffold that facilitates cellular attachment and tissue infiltration; (2) Large pores and channels to facilitate nutrient transport, cellular proliferation, and sustained cellular and tissue viability; (3) An environment compatible for induction of ligamentous differentiation and ingrowth of ligamentous matrix; and (4) A scaffold with the initial mechanical and structural properties to withstand the loading demands within the joint.

Our scaffold was made using the synthetic biomaterial PCLF. This scaffold was initially designed to act in conjunction with two other synthetic polymers, the more rigid biodegradable polypropylene fumarate (PPF) scaffold and poly lactic-co-glycolic acid (PLGA) microspheres, for bone engineering. In a previous investigation, we were able to embed PLGA microspheres containing bone morphogenetic protein-2 (BMP-2) into PPF scaffolds and seeded with bone marrow stromal cells (BMSCs).³³ However, this cytocompatibility was not limited to PPF and PLGA, as PCLF is also very compatible with many different cell types. Given the ability to modify the mechanical properties and geometric properties of PCLF, it is an appealing biomaterial for use in connective tissue engineering applications. Furthermore, it is shown to be slowly degrading *in vivo*, with the structural integrity of the scaffolds remaining intact for well over 16 weeks in most studies.^{17,19,34,35}

PCLF has been previously used as a material in a wide array of biological applications, including injectable scaffolds, drug delivery vehicles, and electrically conductive nerve conduits.^{15–17,19,36–42} By modifying the crystallinity, cross-linking, and degree of polymer branching, the strength, flexibility, and stiffness of PCLF can be modulated.^{19,40,42} For example, the tensile modulus of this polymer can vary from 0.87 to 138 MPa by varying only the molecular weight of the PCL precursor chosen.⁴² Additionally, this

biodegradable material can be sterilized using FDA-approved ethylene oxide or autoclave, with minimal effect on its mechanical properties or cytocompatibility.¹⁹ Using SolidWorks CAD software and SolidScape 3D printer, we were able to create a scaffold with large pores and channels traversing the length of the scaffold with the size and flexibility similar to native human wrist and rabbit ACL ligaments. This is the first description of this novel technique printing a three-dimensional scaffold with customized pore sizes and scaffold geometry.

Important considerations in scaffold engineering involve surface topography, pore size, and biocompatibility. Rougher surfaces with larger pore sizes are generally thought to promote cell attachment and viability, and promote tissue ingrowth when implanted *in vivo*.¹⁷ This represents a challenge in engineering decellularized autograft tendons, as any increase in porosity compromises the tensile strength.^{12,43–47} Furthermore, many natural and synthetic scaffolds have been associated with poor cellular attachment and tissue infiltration secondary to the hydrophobic and acidic nature, and the induction of local inflammatory responses.^{7–11,47} Thus, when considering the use of scaffolds without natural cell binding domains, it is critical to ensure their ability to facilitate cell attachment and cytocompatibility. We created synthetic scaffolds with rougher surfaces and large macro channels traversing the scaffolds in the X, Y, and Z-axes to sustain cellular attachment and growth over 28 days. Additionally, PCLF has been demonstrated in the past to be very compatible with both mature and progenitor nerve and bone cells.^{16,17,40,42} Similar to these studies, the PCLF scaffolds in our study demonstrated good biocompatibility with respect to other cell types from the mesenchymal progeny. The high cell attachment rates and seemingly very friendly micro environment created on the surfaces of these scaffolds lead to the cells proliferating and covering all aspects of the scaffolds after multiple weeks in static culture.

One important finding was that the cells cultured in the presence of growth factors significantly increased cellular proliferation and expression of ligamentous markers. One of the biologic strategies we utilized was PL and the ligamentous differentiation regulator FGF-2. The PL is a collection of lysed platelets from 500 distinct platelet donors from the Mayo Clinic Blood Bank, split into batches containing 8–12 donors according to GMP standards.^{20,21} It has been demonstrated to contain growth factors, such as TGF- β , VEGF, PDGF, FGF, and EGF.²⁰ FGF-2 has been shown to induce stem cell proliferation and differentiation into ligamentous and tenogenic tissues and enhance mechanical strength of such tissues.^{48–50} Similar to prior studies, our results found that PL increases mesenchymal cellular proliferation rates, it does not induce differentiation. Furthermore, PL combined with FGF-2 induced expression of ligamentous matrix proteins, including collagen I, tenascin-C, and collagen III. Further investigation is warranted to determine its potential for augmentation of ligamentous and other mesenchymal tissue regeneration.

In conclusion, we have designed a novel PCLF scaffold using 3D printing to customize a scaffold containing large pores and channels traversing the scaffold in multiple directions. With the aid of a dynamic bioreactor, cells are evenly distributed throughout the scaffold from the first day.

The large pores, rough surface, and cell friendly synthetic polymer creates an environment that progenitor and mature ligamentous cells are able to attach, proliferate, and remain viable for a long period of time. Augmentation with PL and FGF-2 induced adipocyte-derived stem cell proliferation and expression of a ligamentous matrix containing collagen and tenascin-C. In the future, we hope to enhance the potential for clinical translation through investigations into copolymers and other methods of ligamentous differentiation induction using the PCLF scaffold as a backbone. This scaffold has potential within ligament engineering, and the regeneration of many other mesenchymal and skeletal soft tissues.

Disclosure Statement

No competing financial interests exist.

References

1. Watson, H.K., and Ballet, F.L. The SLAC wrist: scapholunate advanced collapse pattern of degenerative arthritis. *J Hand Surg Am* **9**, 358, 1984.
2. Centers for Disease Control, 2003.
3. Nau, T., Lavoie, P., and Duval, N. A new generation of artificial ligaments in reconstruction of the anterior cruciate ligament. Two-year follow-up of a randomised trial. *J Bone Joint Surg Br* **84**, 356, 2002.
4. Benjamin, M., Evans, E.J., and Copp, L. The histology of tendon attachments to bone in man. *J Anat* **149**, 89, 1986.
5. Jackson, D.W., Grood, E.S., Arnoczky, S.P., Butler, D.L., and Simon, T.M. Cruciate reconstruction using freeze dried anterior cruciate ligament allograft and a ligament augmentation device (LAD). An experimental study in a goat model. *Am J Sports Med* **15**, 528, 1987.
6. Woo, S.L., Gomez, M.A., Seguchi, Y., Endo, C.M., and Akeson, W.H. Measurement of mechanical properties of ligament substance from a bone-ligament-bone preparation. *J Orthop Res* **1**, 22, 1983.
7. Bostman, O., and Pihlajamaki, H. Clinical biocompatibility of biodegradable orthopaedic implants for internal fixation: a review. *Biomaterials* **21**, 2615, 2000.
8. Bostman, O.M., and Pihlajamaki, H.K. Adverse tissue reactions to bioabsorbable fixation devices. *Clin Orthop Relat Res* **216**, 2000.
9. Hayashi, M., Zhao, C., An, K.N., and Amadio, P.C. The effects of growth and differentiation factor 5 on bone marrow stromal cell transplants in an *in vitro* tendon healing model. *J Hand Surg Eur Vol* **36**, 271, 2011.
10. Juncosa-Melvin, N., Boivin, G.P., Galloway, M.T., Gooch, C., West, J.R., and Butler, D.L. Effects of cell-to-collagen ratio in stem cell-seeded constructs for Achilles tendon repair. *Tissue Eng* **12**, 681, 2006.
11. Murray, M.M., Spindler, K.P., Abreu, E., Muller, J.A., Nedder, A., Kelly, M., Frino, J., Zurakowski, D., Valenza, M., Snyder, B.D., and Connolly, S.A. Collagen-platelet rich plasma hydrogel enhances primary repair of the porcine anterior cruciate ligament. *J Orthop Res* **25**, 81, 2007.
12. Hoffmann, A., and Gross, G. Tendon and ligament engineering in the adult organism: mesenchymal stem cells and gene-therapeutic approaches. *Int Orthop* **31**, 791, 2007.
13. Shenaq, D.S., Rastegar, F., Petkovic, D., Zhang, B.Q., He, B.C., Chen, L., Zuo, G.W., Luo, Q., Shi, Q., Wagner, E.R., Huang, E., Gao, Y., Gao, J.L., Kim, S.H., Yang, K., Bi, Y., Su, Y., Zhu, G., Luo, J., Luo, X., Qin, J., Reid, R.R., Luu,

- H.H., Haydon, R.C., and He, T.C. Mesenchymal progenitor cells and their orthopedic applications: forging a path towards clinical trials. *Stem Cells Int* **2010**, 519028, 2010.
14. Steinert, A.F., Kunz, M., Prager, P., Barthel, T., Jakob, F., Noth, U., Murray, M.M., Evans, C.H., and Porter, R.M. Mesenchymal stem cell characteristics of human anterior cruciate ligament outgrowth cells. *Tissue Eng Part A* **17**, 1375, 2011.
 15. Jabbari, E., Wang, S., Lu, L., Gruetzmacher, J.A., Ameenuddin, S., Hefferan, T.E., Currier, B.L., Windebank, A.J., and Yaszemski, M.J. Synthesis, material properties, and biocompatibility of a novel self-cross-linkable poly (caprolactone fumarate) as an injectable tissue engineering scaffold. *Biomacromolecules* **6**, 2503, 2005.
 16. Moroder, P., Runge, M.B., Wang, H., Ruesink, T., Lu, L., Spinner, R.J., Windebank, A.J., and Yaszemski, M.J. Material properties and electrical stimulation regimens of polycaprolactone fumarate-polypyrrole scaffolds as potential conductive nerve conduits. *Acta Biomater* **7**, 944, 2011.
 17. Runge, M.B., Dadsetan, M., Baltrusaitis, J., Knight, A.M., Ruesink, T., Lazcano, E.A., Lu, L., Windebank, A.J., and Yaszemski, M.J. The development of electrically conductive polycaprolactone fumarate-polypyrrole composite materials for nerve regeneration. *Biomaterials* **31**, 5916, 2010.
 18. Wang, S., Lu, L., Gruetzmacher, J.A., Currier, B.L., and Yaszemski, M.J. Synthesis and characterizations of biodegradable and crosslinkable poly(epsilon-caprolactone fumarate), poly(ethylene glycol fumarate), and their amphiphilic copolymer. *Biomaterials* **27**, 832, 2006.
 19. Runge, M.B., Wang, H., Spinner, R.J., Windebank, A.J., and Yaszemski, M.J. Reformulating polycaprolactone fumarate to eliminate toxic diethylene glycol: effects of polymeric branching and autoclave sterilization on material properties. *Acta Biomater* **8**, 133, 2012.
 20. Crespo-Diaz, R., Behfar, A., Butler, G.W., Padley, D.J., Sarr, M.G., Bartunek, J., Dietz, A.B., and Terzic, A. Platelet lysate consisting of a natural repair proteome supports human mesenchymal stem cell proliferation and chromosomal stability. *Cell Transplant* **20**, 797, 2011.
 21. Dietz, A.B., Padley, D.J., and Gastineau, D.A. Infrastructure development for human cell therapy translation. *Clin Pharmacol Ther* **82**, 320, 2007.
 22. Su, Y., Wagner, E.R., Luo, Q., Huang, J., Chen, L., He, B.C., Zuo, G.W., Shi, Q., Zhang, B.Q., Zhu, G., Bi, Y., Luo, J., Luo, X., Kim, S.H., Shen, J., Rastegar, F., Huang, E., Gao, Y., Gao, J.L., Yang, K., Wietholt, C., Li, M., Qin, J., Haydon, R.C., He, T.C., and Luu, H.H. Insulin-like growth factor binding protein 5 suppresses tumor growth and metastasis of human osteosarcoma. *Oncogene* **30**, 3907, 2011.
 23. Dadsetan, M., Giuliani, M., Wanivenhaus, F., Brett Runge, M., Charlesworth, J.E., and Yaszemski, M.J. Incorporation of phosphate group modulates bone cell attachment and differentiation on oligo(polyethylene glycol) fumarate hydrogel. *Acta Biomater* **8**, 1430, 2012.
 24. Fan, H., Liu, H., Toh, S.L., and Goh, J.C. Enhanced differentiation of mesenchymal stem cells co-cultured with ligament fibroblasts on gelatin/silk fibroin hybrid scaffold. *Biomaterials* **29**, 1017, 2008.
 25. Canseco, J.A., Kojima, K., Penvose, A.R., Ross, J.D., Obokata, H., Gomoll, A.H., and Vacanti, C.A. Effect on ligament marker expression by direct-contact co-culture of mesenchymal stem cells and anterior cruciate ligament cells. *Tissue Eng Part A* **18**, 2549, 2012.
 26. Rasband, W.S. ImageJ. Bethesda, MD: U. S. National Institutes of Health, 1997–2014. Retrieved from <http://imagej.nih.gov/ij/>
 27. Barrack, R.L., Bruckner, J.D., Kneisl, J., Inman, W.S., and Alexander, A.H. The outcome of nonoperatively treated complete tears of the anterior cruciate ligament in active young adults. *Clin Orthop Relat Res* **192**, 1990.
 28. Fetto, J.F., and Marshall, J.L. The natural history and diagnosis of anterior cruciate ligament insufficiency. *Clin Orthop Relat Res* **29**, 1980.
 29. Petrigliano, F.A., McAllister, D.R., and Wu, B.M. Tissue engineering for anterior cruciate ligament reconstruction: a review of current strategies. *Arthroscopy* **22**, 441, 2006.
 30. Vunjak-Novakovic, G., Altman, G., Horan, R., and Kaplan, D.L. Tissue engineering of ligaments. *Annu Rev Biomed Eng* **6**, 131, 2004.
 31. Freeman, J.W., Woods, M.D., Cromer, D.A., Ekwueme, E.C., Andric, T., Atiemo, E.A., Bijoux, C.H., and Laurencin, C.T. Evaluation of a hydrogel-fiber composite for ACL tissue engineering. *J Biomech* **44**, 694, 2011.
 32. Laurencin, C.T., and Freeman, J.W. Ligament tissue engineering: an evolutionary materials science approach. *Biomaterials* **26**, 7530, 2005.
 33. Kempen, D.H., Kruyt, M.C., Lu, L., Wilson, C.E., Florschutz, A.V., Creemers, L.B., Yaszemski, M.J., and Dhert, W.J. Effect of autologous bone marrow stromal cell seeding and bone morphogenetic protein-2 delivery on ectopic bone formation in a microsphere/poly(propylene fumarate) composite. *Tissue Eng Part A* **15**, 587, 2009.
 34. Daly, W.T., Knight, A.M., Wang, H., de Boer, R., Giusti, G., Dadsetan, M., Spinner, R.J., Yaszemski, M.J., and Windebank, A.J. Comparison and characterization of multiple biomaterial conduits for peripheral nerve repair. *Biomaterials* **34**, 8630, 2013.
 35. Kim, J., Yaszemski, M.J., and Lu, L. Three-dimensional porous biodegradable polymeric scaffolds fabricated with biodegradable hydrogel porogens. *Tissue Eng Part C Methods* **15**, 583, 2009.
 36. Cai, L., and Wang, S. Parabolic dependence of material properties and cell behavior on the composition of polymer networks via simultaneously controlling crosslinking density and crystallinity. *Biomaterials* **31**, 7423, 2010.
 37. Krishna, L., and Jayabalan, M. Synthesis and characterization of biodegradable poly (ethylene glycol) and poly (caprolactone diol) end capped poly (propylene fumarate) cross linked amphiphilic hydrogel as tissue engineering scaffold material. *J Mater Sci Mater Med* **20 Suppl 1**, S115, 2009.
 38. Sharifi, S., Mirzadeh, H., Imani, M., Atai, M., and Ziaee, F. Photopolymerization and shrinkage kinetics of in situ crosslinkable N-vinyl-pyrrolidone/poly(epsilon-caprolactone fumarate) networks. *J Biomed Mater Res A* **84**, 545, 2008.
 39. Sharifi, S., Mirzadeh, H., Imani, M., Rong, Z., Jamshidi, A., Shokrgozar, M., Atai, M., and Roohpour, N. Injectable in situ forming drug delivery system based on poly(epsilon-caprolactone fumarate) for tamoxifen citrate delivery: gelation characteristics, in vitro drug release and anti-cancer evaluation. *Acta Biomater* **5**, 1966, 2009.
 40. Wang, S., Kempen, D.H., Simha, N.K., Lewis, J.L., Windebank, A.J., Yaszemski, M.J., and Lu, L. Photo-cross-linked hybrid polymer networks consisting of poly(propylene fumarate) and poly(caprolactone fumarate): controlled physical properties and regulated bone and nerve cell responses. *Biomacromolecules* **9**, 1229, 2008.

41. Yan, J., Li, J., Runge, M.B., Dadsetan, M., Chen, Q., Lu, L., and Yaszemski, M.J. Cross-linking characteristics and mechanical properties of an injectable biomaterial composed of polypropylene fumarate and polycaprolactone co-polymer. *J Biomater Sci Polym Ed* **22**, 489, 2011.
42. Wang, S., Yaszemski, M.J., Gruetzmacher, J.A., and Lu, L. Photo-crosslinked poly(epsilon-caprolactone fumarate) networks: roles of crystallinity and crosslinking density in determining mechanical properties. *Polymer (Guildf)* **49**, 5692, 2008.
43. Kuo, C.K., Marturano, J.E., and Tuan, R.S. Novel strategies in tendon and ligament tissue engineering: advanced biomaterials and regeneration motifs. *Sports Med Arthrosc Rehabil Ther Technol* **2**, 20, 2010.
44. Omae, H., Zhao, C., Sun, Y.L., An, K.N., and Amadio, P.C. Multilayer tendon slices seeded with bone marrow stromal cells: a novel composite for tendon engineering. *J Orthop Res* **27**, 937, 2009.
45. Vavken, P., Joshi, S., and Murray, M.M. TRITON-X is most effective among three decellularization agents for ACL tissue engineering. *J Orthop Res* **27**, 1612, 2009.
46. Hasslund, S., Jacobson, J.A., Dadali, T., Basile, P., Ulrich-Vinther, M., Soballe, K., Schwarz, E.M., O'Keefe, R.J., Mitten, D.J., and Awad, H.A. Adhesions in a murine flexor tendon graft model: autograft versus allograft reconstruction. *J Orthop Res* **26**, 824, 2008.
47. Altman, G.H., Diaz, F., Jakuba, C., Calabro, T., Horan, R.L., Chen, J., Lu, H., Richmond, J., and Kaplan, D.L. Silk-based biomaterials. *Biomaterials* **24**, 401, 2003.
48. Kimura, Y., Hokugo, A., Takamoto, T., Tabata, Y., and Kurosawa, H. Regeneration of anterior cruciate ligament by biodegradable scaffold combined with local controlled release of basic fibroblast growth factor and collagen wrapping. *Tissue Eng Part C Methods* **14**, 47, 2008.
49. Sahoo, S., Toh, S.L., and Goh, J.C. A bFGF-releasing silk/PLGA-based biohybrid scaffold for ligament/tendon tissue engineering using mesenchymal progenitor cells. *Biomaterials* **31**, 2990, 2010.
50. Yun, Y.R., Won, J.E., Jeon, E., Lee, S., Kang, W., Jo, H., Jang, J.H., Shin, U.S., and Kim, H.W. Fibroblast growth factors: biology, function, and application for tissue regeneration. *J Tissue Eng* **2010**, 218142, 2010.

Address correspondence to:

*Sanjeev Kakar, MD
Mayo Clinic College of Medicine
200 First Street SW
Rochester, MN 55905*

E-mail: kakar.sanjeev@mayo.edu

Received: April 16, 2015

Accepted: July 31, 2015

Online Publication Date: October 30, 2015